Journal of Environmental Management, Volume 270, September 2020, Article number 110887
DOI:10.1016/j.jenvman.2020.110887

Roles of nitrate recycling ratio in the A^2/O - MBBR denitrifying phosphorus removal system for high-efficient wastewater treatment: performance comparison, nutrient mechanism and potential evaluation

Miao Zhang[a], Tianxin Song[a], Chenjie Zhu[a], Yajun Fan[b], Ana Soares[c], Xiaodan Gu[d], Jun Wu[a*]

[a] *College of Environmental Science and Engineering, Yangzhou University, Yangzhou 225127, PR China*

[b] *Yangzhou Polytechnic Institute, Yangzhou 225127, PR China*

[c] *Water Sciences Institute, Cranfield University, Cranfield, MK 43 0AL, UK*

[d] *School of Environmental Science and Engineering, Suzhou University of Science and Technology, Suzhou 215009, China*

*Corresponding author: Jun Wu, College of Environmental Science and Engineering, Yangzhou University, Yangzhou 225127, PR China

E-mail address: j.wu@yzu.edu.cn

Abstract: The long-term effect of nitrate recycling ratios (R=100% - 500%) on the denitrifying phosphorus removal (DPR) characteristics was studied in a novel two-sludge system, which coupled Anaerobic Anoxic Oxic (A^2/O) with Moving Bed Biofilm Reactor (MBBR) for simultaneous nitrogen (N) and phosphorus (P) removals. During the 220 days' operation, effluent COD (30.87 - 45.15 mg/L) can meet the discharge standard completely, but N and P removals were significantly affected by the R-value, including COD_{intra} removal efficiency (COD_{intra}-Re: 56.09 - 85.98%), TN removal (TN-Re: 52.06 - 80.50%), anaerobic PO_4^{3-} release (PO_4^{3-}-An: 10.66 - 29.02 mg/L) and oxic PO_4^{3-} absorption (PO_4^{3-}-O: 2.22 - 6.26 mg/L). Meanwhile, N and P displayed close correlation with the $\Delta PO_4^{3-}/\Delta NO_3^-$ ratio of 4.20 - 4.41 at R=300% - 400%, resulting in the high-efficient anoxic poly-β-hydroxyalkanoates (PHA) utilization (ΔPHA_A: 64.88 mgCOD/gVSS). Based on the stoichiometry methodology, at R of 300% - 400%, the percentages of phosphorus

accumulation organisms (PAOs) and glycogen accumulating organisms (GAOs) contributed to ΔPHA_{An} (ΔGly_{An}) were 71.7%, 28.3% (61.3%, 38.7%) in the anaerobic stage, respectively, while N denitrification rate (NDR_A: 3.91 - 3.93 mgN/(gVSS·h)) and P uptake rate (PUR_A: 3.76 - 3.90 mgP/(gVSS·h)) reached the peak, suggesting superior DPR performance with higher contribution of denitrifying PAOs (DPAOs) (70%) than denitrifying GAOs (DGAOs) (30%) in the anoxic stage. Microbial community analysis showed that *Accumulibacter* (27.66 - 30.01%) was more enriched than *Competibacter* (13.41 - 14.34%) and was responsible for the improved C, N, P removals and DPR characteristics. For optimizing operation, the combined effect of nitrate recycling ratio with other process parameters especially economic evaluation should be considered.

Keywords: A^2/O - MBBR; denitrifying phosphorus removal; nitrate recycling ratio; stoichiometry methodology; microbial community; optimizing operation

1. Introduction

Due to the high operational costs of traditional biological nutrient removal (BNR) process, wastewater treatment plants (WWTPs) are undergoing a shift from nutrient removal to energy-neutral (Ji et al., 2020). Denitrifying phosphorus removal (DPR) had drawn much attention for simultaneous nitrogen (N) and phosphorus (P) removals with one carbon source as electron donor, saving 30% energy requirement and reducing 50% sludge production (Kuba et al., 1996). It was considered as one of the most promising technologies to enrich phosphorus accumulation organisms (PAOs), especially denitrifying PAOs (DPAOs) under the unfavorable condition of low carbon/nitrogen (C/N) ratio wastewater (Zhang et al., 2016a).

Recently, a novel two-sludge process combining A^2/O (Anaerobic Anoxic Oxic) and MBBR (Moving Bed Biofilm Reactor) was developed to strengthen DPR performance (Zhang et al., 2019b). Compared to the traditional DPR processes (e.g., A_2NSBR (Wang et al., 2004), DEPHANOX process (Zafiriadis et al., 2011), A^2/O - BAF (Zhang et al., 2013), etc), A^2/O was conducted in a shorter sludge retention time (SRT) to reinforce DPAOs for efficient DPR, while MBBR with a longer SRT for the enrichment of nitrifying bacteria (including ammonia-oxidizing bacteria (AOB) and nitrite-oxidizing bacteria (NOB)) was operated to achieve complete ammonia (NH_4^+) oxidation. Particularly, suspended carriers with a similar density of water that can move and circulate were added in the MBBR, facilitating the growth of AOB and NOB with slow specific rates (Ahmed et al., 2019).

Notably, as the link between A^2/O and MBBR, nitrate should be returned to the anoxic zones to provide electron acceptor for DPR process via the transformation and utilization of poly-β-hydroxyalkanoates (PHA) and glycogen (Gly) (Zhang et al., 2019a), and to achieve simultaneous high-efficient C, N, P removals. It was reported that lower nitrate recycling ratios could not satisfy high N and P removals, but higher nitrate recycling ratios carried excessive dissolved oxygen (DO) from MBBR to the anoxic zones and suppressed DPAOs activity in the A^2/O reactor (Chen et al., 2015). The reduction of nitrate was used to characterize the bacteria contribution concerning PAOs, DPAOs, glycogen accumulating organisms (GAOs), denitrifying GAOs (DGAOs) as well as ordinary heterotrophic organisms (OHOs) (Wang et al., 2019; Zhang et al., 2019a). More importantly, due to the competition among the above functional groups, it is unclear now how to

balance electron donor, electron acceptor and dominant bacteria for optimal nutrient removal in the A^2/O - MBBR system.

This study focused on the optimization of A^2/O - MBBR system under long-term operation to treat low C/N ratio wastewater by adjusting nitrate recycling ratios. The impact of nitrate recycling ratios on nutrient removals was investigated, where the correlation and evolution of C, N and P performances were analyzed. The specific aim was to evaluate the DPR characteristics, nutrient mechanism and functional bacteria activity based on stoichiometry methodology through batch tests and fluorescence in situ hybridization (FISH) analysis. Finally, the optimized operation strategy for nitrate recycling ratio was elucidated to expedite high-efficient wastewater treatment.

2. Materials and methods

2.1 A^2/O - MBBR process

A novel two-sludge system was developed by integrating A^2/O with MBBR for simultaneous C, N and P removals. Seed sludge taken from Tangwang wastewater treatment plant (Yangzhou, China) was inoculated to achieve the quick start of the A^2/O reactor. The A^2/O reactor (28 L) evenly divided into eight chambers was mainly operated for DPR by high-efficient utilization of influent carbon source. Both anaerobic zones (A_n) and anoxic zones (A_1 - A_6) were equipped with the agitators, and the last chamber of aerobic zone (O) was set to expel nitrogen gas (N_2) with low DO of 1.5 $\pm$ 0.5 mg/L, resulting in the volume ratio as 1:6:1. The A^2/O effluent flowed into middle settler (15 L) for the water and sludge separation. On one side, the supernatant with higher NH_4^+ concentration entered into the MBBR (10.5 L) to complete nitrification. On the other side, the settled sludge was recycled (sludge return ratio: r=100%) into the A^2/O reactor to maintain a stable volatile suspended solids (VSS), while waste sludge was normally discharged to keep a shorter SRT (10 $\pm$ 2 d).

By using the middle settler effluent for incubation, MBBR also realized the quick natural biofilm formation due to the good maneuverability and adaptability (Sun et al., 2019; Zhang et al., 2019b). The main function of MBBR was for nitrification with a longer SRT (> 50 d) (Zhang et al., 2019b), consisting of three identical chambers (N_1, N_2, and N_3) and a small settling zone. It was packed with cylinder polypropylene carriers (size: 5 mm×3 mm, filling ratio: 45%; density: 960 -

1000 kg/m^3; effective porosity: 98%; specific surface area: 1500 m^2/m^3) to avoid the clogging problems (Zhang et al., 2013). DO was controlled around 3.50 ± 0.50 mg/L through flowmeters to ensure efficient contact between substrate and microorganism. According to NH_4^+ loading, aeration in different chambers declined gradually to save energy consumption. The completely oxidized effluent (mainly NO_3^-) acting as the electron acceptor was recycled (nitrate recycling ratio: R=100% - 500%) to A^2/O for the DPR process.

2.2 Wastewater and operation

Domestic sewage collected from a septic tank at the Yangzhou University (Yangzhou, China) was used in this study. The main characteristics of influent were as follows: COD, 206.50 - 295.30 mg/L; NH_4^+, 52.82 - 62.60 mg/L; NO_x^- (NO_2^- + NO_3^-)< 1.0 mg/L, TN, 58.50 - 72.92 mg/L; PO_4^{3-}, 5.24 - 7.38 mg/L, belonging to a typical low C/N ratio (average 3.65) wastewater.

The A^2/O - MBBR was conducted for 220 days divided into five successive phases by adjusting the nitrate recycling ratios (R=100% - 500%): Phase1 (R=100%, 1 - 43 d), Phase2 (R=200%, 44 - 85 d), Phase3 (R=300%, 86 - 130 d), Phase4 (R=400%, 131 - 175 d), and Phase5 (R=500%, 176 - 220 d) (Table 1). The system was operated at room temperature (20 ± 5 °C) with constant hydraulic retention time ($HRT_{A2/O}$=10 h), volume ratio (1:6:1), sludge return ratio (r=100%), and stable biomass in anaerobic zone (6490 - 6953 mg/L) and MBBR (1650 - 1835 mg/L) throughout the operational period. However, due to different nitrate recycling ratios, the effective reaction time in the anoxic zones (HRT_A) shortened from 3.75 to 1.25 h, NO_3^- loading increased from 0.063 to 0.258 kgN/(m^3·d), and VSS_A (VSS_O) declined from 3584 to 1436 mg/L.

2.3 Anaerobic-anoxic/oxic batch tests

Batch experiments involving “Anaerobic-anoxic” with NO_3^- as the electron acceptor and “Anaerobic-oxic” with the O_2 as electron acceptor in each phase (Day 40, Day 80, Day 125, Day 170, and Day 215) (Table 1) were carried out to elucidate nutrient removal mechanism according to our previous methods (Zhang et al., 2016b). Tested sludge taken out from the middle settler was cleaned and centrifuged with deionized water to eliminate the effect of residual substances.

Anaerobic stirring (120 min) was conducted in a sealed reactor (5 L) and the average VSS was set at 3000 ± 200 mg/L by mixing with deionized water. Carbon source (COD: 250 ± 10 mg/L) supplied by sodium acetate was added to finish P release, and carbon utilization rate (CUR, mgCOD/(gVSS·h)) and P release rate (PRR, mgP/(gVSS·h)) were described in Eq. (1) - (2):

$$CUR = \frac{C_{An,T1} - C_{An,T2}}{(T_2 - T_1) \times VSS} \quad (1)$$

$$PRR = \frac{P_{An,T2} - P_{An,T1}}{(T_2 - T_1) \times VSS} \quad (2)$$

where, $C_{An,T1}$, $C_{An,T2}$, $P_{An,T1}$, $P_{An,T2}$ were the COD and PO_4^{3-} concentrations at time T_1 and T_2 under the anaerobic stage, respectively, mg/L.

After the anaerobic reaction, the mixture was halved and placed into two identical reactors (2.5 L), and one was operated aerobically with DO of 3.0 - 4.0 mg/L, while the other reactor was under anoxic condition for DPR with the initial NO_3^- concentration of 30 ± 2 mg/L. P uptake tests lasted 150 min, accompanying by NO_3^- denitrification demonstrated by N denitrification rate (NDR_A, mgN/(gVSS·h)) in Eq.3. Furthermore, it has been confirmed that PAOs were more active with O_2 as the electron acceptor (Hu et al., 2003), and the proportion of DPAOs in PAOs can also be characterized by the ratio of anoxic P uptake rate (PUR_A, mgP/(gVSS·h)) to oxic P uptake rate (PUR_O, mgP/(gVSS·h)) (Eq. (4 - 6)).

$$NDR_A = \frac{N_{A,T1} - N_{A,T2}}{(T_2 - T_1) \times VSS} \quad (3)$$

$$PUR_A = \frac{P_{A,T1} - P_{A,T2}}{(T_2 - T_1) \times VSS} \quad (4)$$

$$PUR_O = \frac{P_{O,T1} - P_{O,T2}}{(T_2 - T_1) \times VSS} \quad (5)$$

$$\text{DPAOs/PAOs}(\%) = PUR_A / PUR_O \quad (6)$$

where, $N_{A,T1}$, $N_{A,T2}$ were the NO_3^- concentrations at time T_1 and T_2 under the anoxic stage, while $P_{A,T1}$, $P_{A,T2}$, $P_{O,T1}$, $P_{O,T2}$ were the PO_4^{3-} concentrations at time T_1 and T_2 under the anoxic and oxic stages, respectively, mg/L.

2.4 Analytical methods

COD quick-analysis apparatus (LH-3C, Lanzhou, China) was used to measure COD concentration, and TN (including NH_4^+, NO_3^-, and NO_2^-), PO_4^{3-}, and VSS were determined according to the standard methods (AWWA, 2005). To identify DPR characteristics, sludge samples in anaerobic-anoxic/oxic batch tests were collected and freeze-dried for PHA and Gly analysis. PHA was performed by a gas chromatographer (Agilent 6890N) using the modified method (Oehmen et al., 2005), while Gly was conducted with the Anthrone method (Zhang et al., 2019a). Data process and correlation analysis were performed by the Origin 2016 software.

The FISH analysis was performed by a digital imaging microscope (OLYMPUS-DP72, Japan) combining with Image-Pro Plus 6.0 to quantitate microbial evolution of PAOs and GAOs on Day 40, Day 80, Day 125, Day 170, and Day 215 (Table 1). The oligonucleotide FISH probes used in this study involved EUB_{mix} (including EUB338, EUB338-II, and EUB338-III) for most *Bacteria*, PAO_{mix} (including PAO462, PAO651, and PAO846) for most *Accumulibacter*, Acc-I-444 for Cluster I of *Accumulibacter*, Acc-II-444 for Cluster II of *Accumulibacter*, GAO_{mix} (including GAO431 and GAO989) for most *Competibacter*, and TFO-DF218, TFO-DF618 for Cluster I of *Defluviicoccus* (Zhang et al., 2020).

3. Results and discussions

3.1 Effect of nitrate recycling ratios on the nutrient removal

3.1.1 The overall performance at various nitrate recycling ratios

Although the influent COD fluctuated between 185.44 and 307.19 mg/L, nitrate recycling ratios exerted a negligible effect on COD removals of the whole A^2/O - MBBR system with a stable COD removal (COD-Re) of 85.66 - 88.79% (Fig.1a), and the effluent (30.87 - 45.15 mg/L) completely met the Class A limit. However, due to the increase of nitrate recycling ratios, the average intracellular carbon storage (COD_{intra}) (Wang et al., 2019) rose from 101.78 mg/L (R=100%) to 143.40 mg/L (R=300%), and appeared a watershed of 155.64 mg/L at R=400%, then declined to 80.16 mg/L (R=500%). Accordingly, the COD_{intra} efficiencies (COD_{intra}-Re, referring to the percentage of COD_{intra} in total anaerobic COD removal) were 56.09%, 67.24%, 82.10%, 85.98%, and 57.48%, respectively, which were similar to the endogenous partial

denitrification and DPR (EPDPR) system (60.6% - 80.1%) (Tenno et al., 2018). The results suggested the significant impact of nitrate recycling ratios on internal PHA storage in the anaerobic zone (Wong et al., 2018b), although NO_3^- was recycled to the anoxic zone.

The NH_4^+ effluent (NH_4^+-eff) were 4.59, 3.82, 2.67, 1.26, 1.39 mg/L, showing positive NH_4^+ removals (NH_4^+-Re) when the nitrate recycling ratios increased (Fig.1b). Specially, due to the dilution effect, NH_4^+-Re increased from 91.18 - 92.65% (R=100%, 200%) to 95.54 - 98.27% (R=300% - 500%), and resulted in a lower NH_4^+ residue in the effluent, revealing obvious superiority in two-sludge systems including traditional A_2SBR (92%) (Kuba et al., 1996) and modified AOA system (95.84%) (Zhao et al., 2018c). Under the similar C/N ratios (3.64 - 3.77), TN removals (TN-Re) improved from 52.06% (R=100%) to 80.50% (R=400%), and TN effluent (including NH_4^+, NO_3^-, NO_2^-) dropped from 30.68 mg/L to 10.87 mg/L. DPAOs cannot compete with OHOs unless the NO_3^- loading exceeds the denitrification potential (Zhang et al., 2016a), so it was adverse for TN removal at lower R with limited NO_3^- loading (0.063 - 0.108 kgN/(m^3·d)). However, when R soared to 500%, TN removal unexpectedly failed with surplus NO_3^- loading (0.258 kgN/(m^3·d)), sliding from 79.81% to 68.69% with higher TN effluent of 20.69 mg/L. It was considered that the presence of excess NO_3^- motivated the activity of OHOs for extracellular denitrification rather than DPAOs for DPR (Saad et al., 2016).

PO_4^{3-} removals (PO_4^{3-}-Re) were also significantly influenced by nitrate recycling ratios (Fig.1c). The anaerobic PO_4^{3-} release (PO_4^{3-}-An) varied from 21.70 mg/L to 29.40 mg/L at R of 100% - 400%, but a higher R of 500% led to the deterioration of PO_4^{3-}-Re. On the one hand, PO_4^{3-}-An was 18.14 mg/L and further decreased to 10.66 mg/L with PO_4^{3-}-Re of 86.38% at R= 500%, while PO_4^{3-}-Re was as high as 94.57 - 95.82% with PO_4^{3-} effluent of 0.24 - 0.32 mg/L at R=300 - 400%. It was reported that more NO_3^- contributed to the competition of carbon sources between PAOs and denitrifiers (Chen et al., 2015), and inhibited the PO_4^{3-}-An. On the other hand, the main functional roles for PO_4^{3-} removal in the anoxic zones (ΔPO_4^{3-}-A) and oxic zone (ΔPO_4^{3-}-O) were different. Under R of 300 - 400%, ΔPO_4^{3-}-O was much lower (2.22 - 2.83 mg/L) and only accounted for 7.65 - 9.62 % of the total PO_4^{3-} uptake, but ΔPO_4^{3-}-O reached to 4.75 - 6.26 mg/L in the other three phases. Higher ΔPO_4^{3-}-O stimulated the activity of PAOs more easily and made it more difficult

for DPAOs to be dominant (Hu et al., 2002). More importantly, PO_4^{3-} deterioration occurred with declined TN-Re after 20 days' operation at R= 500% (Fig.1b), demonstrating the inhibited DPR performance with excess NO_3^- loading.

3.1.2 Correlation analysis at various nitrate recycling ratios

Based on the long-term continuous operation over 220 days, the data correlation at various nitrate recycling ratios was further analyzed (Fig.2). Above all, PO_4^{3-}-An strongly depended on COD_{intra}-Re at R=300% (R^2=0.91, p<0.01) and R=400% (R^2=0.89, p<0.01), while the other three phases were less correlated at R=200% (R^2=0.78, p<0.01) and R=100% (R^2=0.67, p<0.01), especially at R=500% (R^2=0.30, p<0.01) without evident correlation (Fig.2a). Meanwhile, the higher slope of Phase 3 (0.96, p<0.01) and Phase 4 (0.76, p<0.01) proved the high-efficient COD_{intra}-Re (Fig.1a) with complete PO_4^{3-} release (Fig.1c). Furthermore, the correlation between COD_{intra}-Re, PO_4^{3-}-An and nitrate recycling ratio pointed to the reasonable area with lower nitrate recycling ratio of R=200 - 300% (Fig.2b), which also indirectly confirmed the negative effect of R=500%. It was proved that the more COD_{intra} available could not only recover P release at the anaerobic stage but also improve P uptake at the anoxic/oxic stage (Wang et al., 2015). In the EPDPR process, PO_4^{3-}-An decreased from 30 mg/L to 20 mg/L with the decline of COD_{intra}-Re from 80% to 60%, where the percentage of DPAOs dropped from 79.4% to 40% and resulted in poor P removal (Wang et al., 2019). COD_{intra}-Re varied similarly with PO_4^{3-}-An in PNEDPR-SBR (Zhao et al., 2018b) and DPR-SBR (Zhao et al., 2018a) systems. For example, COD_{intra}-Re and PO_4^{3-}-An both decreased to 71.2% and 3.4 mg/L under shorter SRT (Zhao et al., 2018b), besides, PO_4^{3-}-An increased by 6.1 mg/L (7.7 → 13.8 mg/L) with COD_{intra}-Re varied from 63% to 86.9% (Zhao et al., 2018a).

Nevertheless, NO_3^- provided by nitrate recycling was mainly denitrified through PO_4^{3-} removal, displaying a close correlation between TN-Re and PO_4^{3-}-Re ($R^2 \geq 0.80$, p<0.01) (Fig.2c). However, the slope ($\Delta PO_4^{3-}/\Delta NO_x^-$) varied distinctively, reflecting different DPR capacity and DPAOs activity (Zhang et al., 2016a). At R of 300 - 400%, denitrifying 1 mg NO_3^- consumed 4.20 - 4.41 mg PO_4^{3-} in the anoxic zone, which was much higher than A/O-SBR system (1.12 mg PO_4^{3-}) (Zhou et al., 2010) and integrated fixed-film activated sludge (IFAS) system (1.39 - 2.44 mg PO_4^{3-}) (Pouria et al., 2014). By contrast, other three slopes ($\Delta PO_4^{3-}/\Delta NO_3^-$=2.16, 2.37, 3.36 mg/mg) caused higher ΔPO_4^{3-}-O to improve PAOs

activity rather than DPAOs (Fig.1c), indicating that the maximum DPR capacity and DPAOs activity were suppressed at low R of 100%, and were also constrained when R ascended to 500%. Moreover, TN and PO_4^{3-} removals exhibited the mutual effects triggered by nitrate recycling ratios, and the optimal range assembled at 250% - 400% (Fig.2d), exhibiting the vital roles of nitrate recycling ratios on DPR performance.

3.1.3 Evolution of C、N、P at various nitrate recycling ratios

After the raw water entered the system, COD decreased dramatically and approximately 67.86 - 77.78% COD was primarily utilized in the anaerobic zone at R=200 - 400% (Fig.3b-d), while R=100% and R=500% accounted for 56.8% and 57.34 - 59.50%, respectively (Fig.3a, 3e, 3f). The trend was consistent with the variation of COD_{intra}-Re (Fig.1a) although the percentages were different. PHA and Gly varied distinctively despite the final COD effluent were almost below 50 mg/L. At R=200% - 400% (Fig.3b-d), 96.93 - 113.25 mgCOD/gVSS of PHA was synthesized with PO_4^{3-} releasing up to 26.35 - 29.82 mg/L, but higher NO_3^- loading destroyed the anaerobic environment, which was proved that more than 5 mg/L of NO_3^- inhibited PO_4^{3-} release (Comeau et al., 1986). PO_4^{3-}-An decreased to 19.91 mg/L on Day 190 (Fig.3e) and worsened to 8.6 mg/L on Day 210 (Fig.3f) with the lower PHA content of 68.73 - 84.65 mgCOD/gVSS.

In the anoxic zones, COD was basically below 45 mg/L and kept constant from Anoxic1 to Anoxic6 at lower R of 100% - 400% (Fig.3a-d), but obvious anoxic COD consumption (31.6 - 37.3 mg/L) was observed at R=500%, indicating that exogenous denitrification occurred under higher NO_3^- loading (Fig.3e-f). R=100% - 200% resulted in a deficient NO_3^- loading and only 0.76 - 1.14 mg/L NO_x^- was left over, inducing secondary PO_4^{3-} release in the middle settler and PO_4^{3-} residual of 5.4 - 7.34 mg/L in the Anoxic6 (Fig.3a-b). As thus, only 10.79 - 17.70 mgCOD/gVSS PHA was consumed and 17.69 - 22.67 mgCOD/gVSS Gly was synthesized. However, at higher R of 500% (Fig.3e-f), superfluous NO_x^- (5.95 - 7.95 mg/L, including 0.92 - 1.95 mg/L NO_2^-) caused the incomplete PO_4^{3-} absorption, and 56.85 mgCOD/gVSS PHA was utilized and 41.39 mgCOD/gVSS Gly was formed in the anoxic zones on Day 190, comparing with 41.51 mgCOD/gVSS PHA and 28.6 mgCOD/gVSS Gly in the oxic zone on Day 210, indicating the shift of dominant bacteria from DPAOs to PAOs (Fig.1c). Significantly, at R=300% - 400%, not only efficient NO_x^- denitrification was achieved (2.04 - 2.95 mg/L)

but also the complete PO_4^{3-} absorption (0.76 - 1.09 mg/L) in the Anoxic6, and the anoxic PHA utilization (ΔPHA_A) reached to the peak of 64.88 mgCOD/gVSS with a small residue (20.89 - 22.91 mgCOD/gVSS) to maintain the metabolism of DPAOs (Wang et al., 2009). Thereinto, only 0.63 - 0.86 mg/L PO_4^{3-} was absorbed in the oxic zone with respect to 4.08 - 4.89 mg/L at R=100% - 200% and 2.29 - 3.86 mg/L at R=500%, proving that the short oxic zone was crucial and indispensable in stabilizing P effluent (Zhang et al., 2016a).

In the MBBR, 23.6 mg/L COD (others: 3.93 - 8.20 mg/L) was degraded on Day 210 (Fig.3f), which depressed the growth of AOB and NOB owing to the higher proliferation rate of OHOs (Zhang, 2000). From the view of COD, nitrate recycling ratios not only worked upon the DPR performance in A^2/O but also affected the nitrifiers in MBBR although the VSS was only 1655 - 1835 mg/L (Table 1). In particular, slight nitrite accumulation (NO_2^-: 0.93 - 1.68 mg/L) occurred during nitrification, but the microbial competition between AOB and NOB should be optimized to promote high nitrite accumulation for saving carbon source and aeration consumption (Zhang et al., 2019b). Moreover, simultaneous nitrification and denitrification (SND) (8.41 - 13.65%) (Fig.3a-d) was also observed although DPR was the main nitrogen metabolic pathway. It was easy to shape local anoxic/anaerobic environment especially inner the thicker biofilm layer during O_2 transferring (Gong et al., 2012), and enhancing SND could be another alternative to achieve deep-level DPR under higher nitrate recycling ratios.

3.2 Nutrient removal mechanism linked with DPR

3.2.1 DPR characteristics in the typical anaerobic-anoxic/oxic batch tests

Batch tests were carried out to elucidate DPR characteristics, such as substrate transformation and utilization of COD, NO_3^-, PO_4^{3-}, PHA, and Gly. During the anaerobic stirring, COD decreased rapidly and was stored in the form of PHA while Gly was degraded to provide energy for P release (Zhang et al., 2019a). However, nutrient variations differed with the long-term effect of nitrate recycling ratios (Fig.4). COD was high-efficiently utilized with a little surplus of 46.2 - 52.7 mg/L and PO_4^{3-}-An reached to 23.27 (R=100%), 28.45 - 32.91 mg/L (R=200 - 400%), while 100.36 mg/L COD was left and PO_4^{3-}-An was only 15.6 mg/L at higher R of 500% (Fig.4a-b). Accordingly, the synthetic PHA increased from 45.4 - 50.2

mgCOD/gVSS to 113.4, 124.45 - 140.91 mgCOD/gVSS with Gly decomposition of 98.9, 126.8 - 153.2 mgCOD/gVSS at R=100%, R=200 - 400%, respectively, comparing with small amount of PHA (35.50 mgCOD/gVSS) was synthesized and Gly (79.64 mgCOD/gVSS) was consumed at R=500% (Fig.4c).

To better explain anaerobic mechanism, two distinct processes with various metabolic rates were compared because of different reaction driving force (Wong et al., 2018a; Wong et al., 2018b). Faster CUR during the first 60 min (49.78 - 58.29 mgCOD/(gVSS·h)) contributed to a higher ΔPHA_{An} (68.85 - 79.35 mgCOD/gVSS) and PRR (8.18 - 8.53 mgP/ (gVSS·h)), while PRR dropped to 1.54 - 2.03 mgP/(gVSS·h) owing to the lower CUR (13.71 - 17.35 mgCOD/(gVSS·h)) and ΔPHA_{An} (15.53 - 18.68 mgCOD/gVSS) during the last 60 min, demonstrating a close relation between COD_{intra}-Re and PO_4^{3-}-An at R=300 - 400% (Fig.2a-b). It's worth noting that the anaerobic metabolic activity of CUR, ΔPHA_{An} and PRR at R=100% (37.87/22.82 mgCOD/(gVSS·h), 50.50/17.50 mgCOD/gVSS, 5.18/2.27 mgP/(gVSS·h)) was inferior to R=200% (40.94/24.16 mgCOD/(gVSS·h), 53.27/22.97 mgCOD/gVSS, 6.86/2.45 mgP/(gVSS·h)), but superior to R=500% (27.26/21.01 mgCOD/(gVSS·h), 25.20/10.30 mgCOD/gVSS, 2.95/2.05 mgP /(gVSS·h)), which led to the exasperated COD_{intra} and PO_4^{3-}-An (Fig.1). The results initially showed that the bioactivity has been changed by the long-term impact of nitrate recycling ratios.

As the main area for DPR, the variation of NO_3^- coupling with PO_4^{3-} in the anoxic stage was exhibited in Fig.4d. Unlike the continuous operation, equal initial NO_3^- (30 $\pm$ 2 mg/L) and reaction time (150 min) were performed, but 3.67 - 5.1 mg/L NO_3^- and 5.8 - 6.5 mg/L PO_4^{3-} were remained at Phase 1 - 2, while NO_3^- (0.35 - 0.86 mg/L) and PO_4^{3-} (1.90 - 2.41 mg/L) were both efficiently removed at Phase 3 - 4. NDR increased from 3.28 - 3.45 mgN/(gVSS·h) (Phase 1 - 2) to 3.91 - 3.93 mgN/(gVSS·h) (Phase 3 - 4), while PUR_A (3.76 - 3.90 mgP/(gVSS·h)) and ΔPHA_A (112.75 - 114.51 mgCOD/(gVSS·h)) achieved the optimal range on Day 125 and Day 170. Particularly, NDR and PUR_A fell to 1.81 mgN/(gVSS·h), 1.72 mgP/(gVSS·h) with ΔPHA_A of 84.34 mgCOD/(gVSS·h) on Day 215, and Gly reached to the peak of 182.9 mgCOD/(gVSS·h) but declined by 47.3 mgCOD/(gVSS·h) during the last 90 min (Fig.4e), which resulted in microbial starvation and DPAOs repression (Bassin et al., 2012) with the depletion of PHA (residual amount: 20.33

mgCOD/(gVSS·h)).

Furthermore, PAOs excessively absorbed PO_4^{3-} with much higher PUR_O (4.08 - 4.93 mgP/(gVSS·h)) than PUR_A (1.72 - 3.90 mgP/(gVSS·h)), contributing to more ΔPHA_O (73.05 - 123.06 mgCOD/(gVSS·h)) than ΔPHA_A (67.06 - 114.51 mgCOD/(gVSS·h)). Unlike the anoxic stage, PO_4^{3-} was completely absorbed within 90 min and the linear relation between PO_4^{3-} and reaction time fitted well (regression coefficients $R^2 \geq 0.83$) in the oxic stage (Fig.4f). In terms of slopes, the highest value on Day 215 (0.27> 0.16 - 0.20) suppressed DPAOs activity, and the relative ratios of DPAOs/PAOs increased from 46.9% (Day 40) to 93.5% (Day 170) but reduced to 34.9% (Day 215), causing the deteriorative nutrient removals (Fig.1). According to our previous research (Zhang et al., 2016a), sufficient metabolic energy and suitable NO_3^- loading were both responsible for DPAOs growth.

3.2.2 Stoichiometry methodology of functional microbial activity

Functional microbial activity (e.g. PAOs, DPAOs, GAOs, DGAOs) based on the stoichiometry methodology was further analyzed (Table 2). During the anaerobic stage (120 min), PRR/CUR from Phase 1 to Phase 4 (0.19 - 0.25 molP/molC) was similar with our previous study (0.27 molP/molC) (Zhang et al., 2019a) and EPDPR system (0.21 molP/molC) (Wang et al., 2019), but much lower than the reported PAOs model (0.50 molP/molC) (Wang et al., 2016). The lowest PRR/CUR (0.12 molP/molC) in Phase 5 indicated that GAOs rather than PAOs played a major role in carbon utilization. The peaks of $\Delta PHA/COD_{intra}$ (1.48 molC/molC) and $\Delta Gly/COD_{intra}$ (0.74 molC/molC) were higher than the PAOs mode value (1.33, 0.50 molC/molC) (Wang et al., 2016) but significantly lower than the GAOs mode value (1.86, 1.12 molC/molC) (Zeng et al., 2003a). According to the metabolism model, under R=300 - 400%, the percentage of PAOs contributed to ΔPHA_{An} was 71.7% ((1.86-1.48) molC/molC/(1.86-1.33) molC/molC ×100%) while GAOs' contribution accounted for 28.3%. Similarly, the proportion of PAOs contributed to ΔGly_{An} was 61.3% ((1.12-0.74) molC/molC/(1.12-0.5) molC/molC×100%) while GAOs' contribution accounted for 38.7%.

During the anoxic stage (150 min), $\Delta PO_4^{3-}/\Delta PHA$ (0.06 - 0.17 molP/molC) was higher than the DPAOs model value (0.06 molP/molC), and the maximum $\Delta PO_4^{3-}/\Delta PHA$ contributed to the optimal PUR_A (3.76 - 3.90 mgP/(gVSS·h)) under

R=300% - 400%. $\Delta NO_3^-/\Delta PHA$ (0.65, 0.52 molN/molC) under R=100 - 400% was higher than the DPAOs model (0.40 molN/molC) (Wang et al., 2019) but coincident with the DGAOs model (0.80 molN/molC) (Ji et al., 2019). Particularly, under R=100 - 200% and R=300 - 400%, the percentages of DPAOs contributed to ΔNO_3^- were 37.5% ((0.8-0.65) molN/molC/(0.8-0.4) molN/molC×100%), 70% ((0.8-0.52) molN/molC/ (0.8-0.4) molN/molC×100%) with DGAOs' contributing to 62.5%, 30%, respectively, showing the shift of functional bacteria caused by nitrate recycling ratios. However, $\Delta NO_3^-/\Delta PHA$ (0.14 molN/molC) in Phase 5 was much lower than both DPAOs and DGAOs models, confirming the existence of extracellular denitrification under higher NO_3^- loading (Fig.1). ΔGly/ΔPHA (0.63 - 0.76 molC/molC) in Phase 1 - 4 approached the DGAOs model values (0.63 molC/molC (Zeng et al., 2003b), 0.69 molC/molC (Ji et al., 2019)) but higher than the DPAOs model value (0.52 molC/molC), indicating DPAOs and DGAOs were both responsible for PHA consumption and Gly synthesis. ΔGly/ΔPHA in Phase 5 (- 0.36 molC/molC) proved the microbial starvation by consuming Gly to remedy PHA (Fig.4), although the DGAOs model by utilizing Gly should be further explored when PHA was depleted (Miao et al., 2015).

During the oxic stage (150 min), $\Delta PO_4^{3-}/\Delta PHA$ (0.10 - 0.16 molP/molC) was lower than the reported PAOs model (0.41 molP/molC) (Smolders et al., 1994), and ΔGly/ΔPHA (0.45 - 0.92 molC/molC) was close to the anaerobic/aerobic system (0.95 molC/molC) but obviously higher than the PAOs model (0.42 molC/molC) (Smolders et al., 1994) and EPDPR system (0.57 molC/molC) (Wang et al., 2019). Thus, GAOs were dominant in oxic PHA and Gly transformation and PAOs were mainly responsible for P uptake using both O_2 and NO_3^- as electron acceptor (Peng et al., 2006).

3.2.3 Microbial community evolution

Microbial activity and population quantification were compared using some representative images in Phase 1 (Day 40), Phase 3 (Day 125) and Phase 5 (Day 215) (Fig.5a-l), and the specific distributions of PAOs and GAOs revealed the evolution rule (Fig.5m). With the augment of R from 100% to 400%, PAOs belonging to *Accumulibacter* increased from 6.48 ± 0.86% (Day 40) to 15.85 ± 1.05% (Day 80), 27.66 ± 1.07% (Day 125), 30.01 ± 0.93% (Day 170), with 86.88 - 92.63% belonging to Cluster I. Although GAOs in terms of *Competibacter* showed the same upward trends from 3.65 ±

0.65% (Day 40) to 4.02 ± 0.26% (Day 80), 13.41 ± 1.25% (Day 125), 14.34 ± 0.91% (Day 170), the enriched PAOs group taking the absolute advantage than GAOs was responsible for the better nutrient removals (Fig.1, Fig.3) and DPR characteristics (Fig.4, Table 2).

In Phase 5, PAOs (mainly Cluster I of *Accumulibacter*) and GAOs (including *Competibacter* and Cluster I of *Defluviicoccus*) accounted for 2.35 ± 0.25%, 27.83 ± 1.23%, respectively. Comparing with Phase 4, the decrease in PAOs population (~27.66%) and the increase in GAOs population (~12.61%) led to the deterioration of C, N, and P removals (Fig.1, Fig.3). Thus, the shift of PAOs and GAOs was strongly related to the DPR performance and nutrient mechanism. Specially, the minor enriched PAOs group (Cluster II of *Accumulibacter*) only accounted for 0.06 - 0.26% through the whole operation. In contrast, *Defluviicoccus* responsible for NO_2^- accumulation (Zhang et al., 2020) maintained a steady percentage of 0.65 - 1.07% in Phase 1 - 4 but ascended to 4.66 ± 0.21% in Phase 5, confirming the NO_3^--to-NO_2^- transformation (Fig.3e-f). The possible reason could be due to the incomplete denitrification under higher NO_3^- loading (Wang et al., 2019), but further studies are still needed since high NO_2^- levels might suppress bioactivity.

3.3 Optimizing operation for high-efficient wastewater treatment

A^2/O coupling with MBBR could achieve high-efficient C, N, P removals by optimizing nitrate recycling ratios from low C/N ratio wastewater. It was recognized that lower R (100% - 200%) reduced electron acceptor of NO_3^- and restricted DPR performance with higher potential risk for secondary P release (Zhang et al., 2016a). On the contrary, higher R (500%) bringing excessive DO and NO_3^- inhibited DPAOs activity (Chen et al., 2015) and promoted the adverse growth of OHOs (Fig.3). Fortunately, R=300 - 400% not only allowed efficient PHA synthesis and utilization with higher COD_{intra}-Re (82.10 - 85.98%), TN-Re (78.26 - 80.50%) and PO_4^{3-}-Re (94.57 - 95.82%) (Fig.1) but also maintained superior DPR characteristics, microbial activity (Table 2), and enriched functional bacteria (*Accumulibacter*: 27.66 - 30.01%. vs. *Competibacter*: 13.41 - 14.34%) (Fig.5). The conclusion was consistent with the A^2/O - BAF system under the combined effects of C/N ratios and nitrate recycling ratios (Chen et al., 2015).

More importantly, A^2/O - MBBR showed many considerable advantages over the traditional enhanced biological

phosphorus removal (EBPR) systems, which provided the potential to upgrade and retrofit the existing WWTPs. Firstly, the longer anaerobic/anoxic operation rather than anaerobic/oxic condition strengthened DPR performance and DPAOs enrichment, saving operating cost and aeration consumption (Wong et al., 2018b). Secondly, DPR achieved the simultaneous N and P removals using the same carbon source without external carbon addition, especially for low C/N ratio wastewater treatment (Zhang et al., 2019a). Finally, the superior DPR performance accelerated the formation of granular sludge contributing to higher shock resistance (Zhang et al., 2020), and the better settleability with higher P content provided feasibilities for P recovery and reuse (Yuan et al., 2012).

However, there are still many aspects to be fully addressed. According to the metabolism theory of PAOs and GAOs (Lopez-Vazquez et al., 2009), electron acceptor by adjusting nitrate recycling ratios should be controlled in appropriate concentration and below inhibition level. Due to the specific operation parameters in this study (Table 1), the nutrient removals still need to be optimized and improved for advanced wastewater treatment (Du et al., 2019), and the combined effects of HRTs, volume ratios and C/N ratios with R should also be conducted. For example, the optimal R may increase to 500% or 600% with longer HRT or extended anoxic reaction time, but it will bring high pumping electric cost. In this regard, both nutrient performance and economic evaluation should be considered in the real application.

4. Conclusions

A^2/O - MBBR system based on DPR was successfully operated by optimizing nitrate recycling ratios to treat low C/N ratio wastewater, and R=300% - 400% was proved as a watershed for nutrient removal. R exerted a negligible effect on the overall COD removals (85.66 - 88.79%) but induced significant COD_{intra}-Re (56.09 - 85.98%), which further generated a strong relation between PO_4^{3-}-An and COD_{intra}-Re. Moreover, the correlation and evolution of nutrients not only described the roles of oxic zone in stabilizing PO_4^{3-}-P effluent as well as anoxic zone in NO_2^- accumulation but also proved SND in the MBBR. Batch tests elucidated DPR characteristics associated with CUR, PRR, PUR, and NDR, while stoichiometry analysis evaluated PHA and Gly transformation linked with microbial activity. Furthermore, the shift of main functional bacteria (*Accumulibacter*-PAOs and *Competibacter*-GAOs) was proved to be strongly related to the DPR performance and

nutrient mechanism. The operation strategy coupling deep-level nutrient removal with economic evaluation was further proposed.

Acknowledgments

This research was financially supported by the Natural Science Foundation of China (Grant No. 51808482), Natural Science Foundation of Jiangsu Province (Grants No. BK20170506), and Postdoctoral Science Foundation (Grants No. 2018M632392).

Appendix A. Supplementary data

Supplementary data associated with A^2/O - MBBR schematic diagram, DPR characteristics in batch tests can be found in the online version.

References

Ahmed, W., Tian, X., Delatolla, R. 2019. Nitrifying moving bed biofilm reactor: Performance at low temperatures and response to cold-shock. *Chemosphere*, **229**, 295-302.

AWWA. 2005. *Standard Methods for the Examination of Water and Wastewater. 21st ed*. American Water Works Association.

Bassin, J.P., Kleerebezem, R., Dezotti, M., van Loosdrecht, M.C. 2012. Simultaneous nitrogen and phosphate removal in aerobic granular sludge reactors operated at different temperatures. *Water Research*, **46**(12), 3805-3816.

Chen, Y., Li, B., Ye, L., Peng, Y. 2015. The combined effects of COD/N ratio and nitrate recycling ratio on nitrogen and phosphorus removal in anaerobic/anoxic/aerobic (A 2 /O)-biological aerated filter (BAF) systems. *Biochemical Engineering Journal*, **93**(10), 235-242.

Comeau, Y., Hall, K.J., Hancock, R.E.W., Oldham, W.K. 1986. Biochemical model for enhanced biological phosphorus removal. *Water Research*, **20**(12), 1511-1521.

Du, S., Yu, D., Zhao, J., Wang, X., Bi, C., Zhen, J., Yuan, M. 2019. Achieving deep-level nutrient removal via combined denitrifying phosphorus removal and simultaneous partial nitrification-endogenous denitrification process in a single-sludge sequencing batch reactor. *Bioresource Technology*, **289**, 121690.

Gong, L., Jun, L., Yang, Q., Wang, S., Ma, B., Peng, Y. 2012. Biomass characteristics and simultaneous nitrification–denitrification under long sludge retention time in an integrated reactor treating rural domestic sewage. *Bioresource technology*, **119**, 277-284.

Hu, J.Y., Ong, S.L., Ng, W.J., Lu, F., Fan, X.J. 2003. A new method for characterizing denitrifying phosphorus removal bacteria by using three different types of electron acceptors. *Water Research*, **37**(14), 3463-3471.

Hu, Z.-r., Wentzel, M.C., Ekama, G.A. 2002. Anoxic growth of phosphate-accumulating organisms (PAOs) in biological nutrient removal activated sludge systems. *Water Research*, **36**(19), 4927-4937.

Ji, J., Peng, Y., Li, X., Zhang, Q. 2019. Stable long-term operation and high nitrite accumulation of an endogenous partial-denitrification (EPD) granular sludge system under mainstream conditions at low temperature. *Bioresource Technology*, **289**, 121634.

Ji, J., Peng, Y., Wang, B., Li, X., Zhang, Q. 2020. A novel SNPR process for advanced nitrogen and phosphorus removal from mainstream wastewater based on anammox, endogenous partial-denitrification and denitrifying dephosphatation. *Water Research*, **170**, 115363.

Kuba, T., van Loosdrecht, M.C.M., Heijnen, J.J. 1996. Phosphorus and nitrogen removal with minimal COD requirement by integration of denitrifying dephosphatation and nitrification in a two-sludge system. *Water Research*, **30**(7), 1702-1710.

Lopez-Vazquez, C.M., Oehmen, A., Hooijmans, C.M., Brdjanovic, D., Gijzen, H.J., Yuan, Z., van Loosdrecht, M.C.M. 2009. Modeling the PAO–GAO competition: Effects of carbon source, pH and temperature. *Water Research*, **43**(2), 450-462.

Miao, L., Wang, S., Li, B., Cao, T., Xue, T., Peng, Y. 2015. Advanced nitrogen removal via nitrite using stored polymers in a modified sequencing batch reactor treating landfill leachate. *Bioresource Technology*, **192**, 354-360.

Oehmen, A., Keller-Lehmann, B., Zeng, R.J., Yuan, Z., Keller, J. 2005. Optimisation of poly-β-hydroxyalkanoate analysis using gas chromatography for enhanced biological phosphorus removal systems. *Journal of Chromatography A*, **1070**(1), 131-136.

Peng, Y.-z., Wang, X.-l., Li, B.-k. 2006. Anoxic biological phosphorus uptake and the effect of excessive aeration on biological phosphorus removal in the A2O process. *Desalination*, **189**(1), 155-164.

Pouria, Jabari, Giulio, Munz, Jan, A., Oleszkiewicz. 2014. Selection of denitrifying phosphorous accumulating organisms in \\{IFAS\\} systems: Comparison of nitrite with nitrate as an electron acceptor. *Chemosphere*, **109**, 20-27.

Saad, S.A., Welles, L., Abbas, B., Lopez-Vazquez, C.M., van Loosdrecht, M.C.M., Brdjanovic, D. 2016. Denitrification of nitrate and nitrite by 'Candidatus Accumulibacter phosphatis' clade IC. *Water Research*, **105**, 97-109.

Smolders, G.J., Meij, J., Van Der, Loosdrecht, M.C., Van, Heijnen, J.J. 1994. Model of the anaerobic metabolism of the biological phosphorus removal process: Stoichiometry and pH influence. *Biotechnology & Bioengineering*, **43**(6), 461-470.

Sun, S., Jia, T., Chen, K., Peng, Y., Zhang, L. 2019. Simultaneous removal of hydrogen sulfide and volatile organic sulfur

compounds in off-gas mixture from a wastewater treatment plant using a two-stage bio-trickling filter system. *Frontiers of Environmental Science & Engineering*, **13**(4), 60.

Tenno, T., Rikmann, E., Zekker, I., Tenno, T. 2018. Modelling the solubility of sparingly soluble compounds depending on their particles size. *Proceedings of the Estonian Academy of Sciences*, **67**(3), 300-302.

Wang, X., Wang, S., Xue, T., Li, B., Xian, D., Peng, Y. 2015. Treating low carbon/nitrogen (C/N) wastewater in simultaneous nitrification-endogenous denitrification and phosphorous removal (SNDPR) systems by strengthening anaerobic intracellular carbon storage. *Water Research*, **77**, 191-200.

Wang, X., Wang, S., Zhao, J., Dai, X., Li, B., Peng, Y. 2016. A novel stoichiometries methodology to quantify functional microorganisms in simultaneous (partial) nitrification-endogenous denitrification and phosphorus removal (SNEDPR). *Water Research*, **95**, 319-329.

Wang, X., Zhao, J., Yu, D., Chen, G., Du, S., Zhen, J., Yuan, M. 2019. Stable nitrite accumulation and phosphorous removal from nitrate and municipal wastewaters in a combined process of endogenous partial denitrification and denitrifying phosphorus removal (EPDPR). *Chemical Engineering Journal*, **355**, 560-571.

Wang, Y., Peng, Y., Stephenson, T. 2009. Effect of influent nutrient ratios and hydraulic retention time (HRT) on simultaneous phosphorus and nitrogen removal in a two-sludge sequencing batch reactor process. *Bioresour Technol*, **99**(14), 3506-3512.

Wang, Y.Y., Peng, Y.Z., Li, T.W., Ozaki, M., Takigawa, A., Wang, S.Y. 2004. Phosphorus removal under anoxic conditions in a continuous-flow A2N two-sludge process. *Water Science & Technology*, **50**(6), 37.

Wong, P.Y., Cheng, K.Y., Krishna, K.C.B., Kaksonen, A.H., Sutton, D.C., Ginige, M.P. 2018a. Improvement of carbon usage for phosphorus recovery in EBPR-r and the shift in microbial community. *Journal of Environmental Management*, **218**, 569-578.

Wong, P.Y., Ginige, M.P., Kaksonen, A.H., Sutton, D.C., Cheng, K.Y. 2018b. The ability of PAOs to conserve their storage-driven phosphorus uptake activities during prolonged aerobic starvation conditions. *Journal of Water Process Engineering*, **23**, 320-326.

Yuan, Z., Pratt, S., Batstone, D.J. 2012. Phosphorus recovery from wastewater through microbial processes. *Curr Opin Biotechnol*, **23**(6), 878-883.

Zafiriadis, I., Ntougias, S., Nikolaidis, C., Kapagiannidis, A.G., Aivasidis, A. 2011. Denitrifying polyphosphate accumulating organisms population and nitrite reductase gene diversity shift in a DEPHANOX-type activated sludge system fed with municipal wastewater. *Journal of Bioscience & Bioengineering*, **111**(2), 185-192.

Zeng, R.J., van Loosdrecht, M.C.M., Yuan, Z., Keller, J. 2003a. Metabolic model for glycogen-accumulating organisms in anaerobic/aerobic activated sludge systems. *Biotechnology and Bioengineering*, **81**(1), 92-105.

Zeng, R.J., Yuan, Z., Keller, J. 2003b. Enrichment of denitrifying glycogen-accumulating organisms in anaerobic/anoxic activated sludge system. *Biotechnology and Bioengineering*, **81**(4), 397-404.

Zhang, M., Peng, Y., Wang, C., Wang, C., Zhao, W., Zeng, W. 2016a. Optimization denitrifying phosphorus removal at different hydraulic retention times in a novel anaerobic anoxic oxic-biological contact oxidation process. *Biochemical Engineering Journal*, **106**, 26-36.

Zhang, M., Wang, C., Peng, Y., Wang, S., Jia, F., Zeng, W. 2016b. Organic substrate transformation and sludge characteristics in the integrated anaerobic anoxic oxic–biological contact oxidation (A2/O–BCO) system treating wastewater with low carbon/nitrogen ratio. *Chemical Engineering Journal*, **283**, 47-57.

Zhang, M., Wang, Y., Fan, Y., Liu, Y., Yu, M., He, C., Wu, J. 2019a. Bioaugmentation of low C/N ratio wastewater: Effect of acetate and propionate on nutrient removal, substrate transformation, and microbial community behavior. *Bioresource Technology*, 122465.

Zhang, M., Yu, M., Wang, Y., He, C., Pang, J., Wu, J. 2019b. Operational optimization of a three-stage nitrification moving bed biofilm reactor (NMBBR) by obtaining enriched nitrifying bacteria: Nitrifying performance, microbial community, and kinetic parameters. *Science of The Total Environment*, **697**, 134101.

Zhang, M., Zhu, C., Pan, T., Fan, Y., Liu, Y., He, C., Gu, X., Wu, J. 2020. Elucidating sludge characteristic, substrate transformation and microbial evolution in a two-sludge denitrifying phosphorus removal system under the impact of

HRT. *Journal of Environmental Management*, **262**, 110391.

Zhang, W., Peng, Y., Ren, N., Liu, Q., Chen, Y. 2013. Improvement of nutrient removal by optimizing the volume ratio of anoxic to aerobic zone in AAO-BAF system. *Chemosphere*, **93**(11), 2859-2863.

Zhang, Z., Lin, R. 2000. Drainage works. *Beijing: China Building Industry Press*, 30-32.

Zhao, J., Wang, X., Li, X., Jia, S., Peng, Y. 2018a. Advanced nutrient removal from ammonia and domestic wastewaters by a novel process based on simultaneous partial nitrification-anammox and modified denitrifying phosphorus removal. *Chemical Engineering Journal*, **354**, 589-598.

Zhao, J., Wang, X., Li, X., Jia, S., Peng, Y. 2018b. Combining partial nitrification and post endogenous denitrification in an EBPR system for deep-level nutrient removal from low carbon/nitrogen (C/N) domestic wastewater. *Chemosphere*, **210**, 19-28.

Zhao, W., Huang, Y., Wang, M., Pan, C., Li, X., Peng, Y., Li, B. 2018c. Post-endogenous denitrification and phosphorus removal in an alternating anaerobic/oxic/anoxic (AOA) system treating low carbon/nitrogen (C/N) domestic wastewater. *Chemical Engineering Journal*, **339**, 450-458.

Zhou, S., Zhang, X., Feng, L. 2010. Effect of different types of electron acceptors on the anoxic phosphorus uptake activity of denitrifying phosphorus removing bacteria. *Bioresource technology*, **101**(6), 1603-1610.

Table captions

Table 1 Operational parameters of the A^2/O - MBBR system in different phases

Table 2 Comparison of intercellular carbon transformation with the model values based on stoichiometry methodology

Table 1 Operational parameters of the A^2/O - MBBR system in different phases

Phase	Duration (d)	R (%)	HRT_A[b] (h)	NO_3^- loading kgN/(m^3·d)	VSS_{An}[c] (mg/L)	VSS_A[c] VSS_O[c] (mg/L)	VSS[d] (mg/L)	Other parameters
1	1 - 43/40[a]	100	3.75	0.063	6780 ± 20	3584 ± 25	1835 ± 26	Average C/N ratio=3.62 $HRT_{A2/O}$=10 h Temperature=20 ± 5℃ Volume ratio=1:6:1 r=100%
2	44 - 85/80[a]	200	2.50	0.108	6875 ± 28	2372 ± 20	1790 ± 15	
3	86 - 130/125[a]	300	1.88	0.127	6490 ± 35	2193 ± 25	1724 ± 22	
4	131 - 175/170[a]	400	1.50	0.164	6528 ± 30	1660 ± 35	1650 ± 35	
5	176 - 220/215[a]	500	1.25	0.258	6953 ± 43	1436 ± 23	1748 ± 20	

a: the dates of batch test and FISH analysis;

b: the effective reaction time in the anoxic zone, $HRT_A=V_A/((1+R)Q)$;

c: the average biomass in the A^2/O reactor (anaerobic zone, VSS_{An}; anoxic zone, VSS_A; oxic zone, VSS_O; $VSS_A \approx VSS_O$);

d: the average biomass in the MBBR.

Table 2 Comparison of intercellular carbon transformation with the model values based on stoichiometry methodology

Anaerobic stage (120 min)			Anoxic stage (150 min)			Oxic stage (150 min)		References
PRR/CUR (molP/molC)	ΔPHA/COD_{intra} (molC/molC)	ΔGly/COD_{intra} (molC/molC)	ΔPO_4^{3-}/ΔPHA (molP/molC)	ΔGly/ΔPHA (molC/molC)	ΔNO_3^-/ΔPHA (molN/molC)	ΔPO_4^{3-}/ΔPHA (molP/molC)	ΔGly/ΔPHA (molC/molC)	
0.21	1.75	1.03	0.06	0.52	0.40	0.27	0.57	Wang et al., 2019
0.27	1.08	0.76	0.07	0.67	0.16	0.05	0.67	Zhang et al., 2019a
0.50	1.33	0.50	0.15	0.30	0.16	-	-	Wang et al., 2016
-	1.86	1.12	-	-	-	-	0.95	Zeng et al., 2003a
-	-	-	-	0.63	0.41	-	-	Zeng et al., 2003b
-	-	-	-	0.69	0.80	-	-	Ji et al., 2019
-	-	-	-	-	-	0.41	0.42	Smolders et al.,1994
0.19	1.14	0.63	0.12	0.63	0.65	0.10	0.45	This study[a] (Phase1,2)
0.25	1.48	0.74	0.17	0.76	0.52	0.12	0.48	This study[a] (Phase3, 4)
0.12	0.88	0.92	0.06	- 0.36	0.14	0.16	0.92	This study (Phase5)

a: the average value.

Figure captions

Fig.1 The overall removal performance in the A^2/O - MBBR system (a: COD; b: TN and NH_4^+; c: PO_4^{3-})

Fig.2 Correlation analysis of DPR characteristics (a, b: COD and PO_4^{3-}; c, d: TN and PO_4^{3-})

Fig.3 Nutrient variations along the reaction zones in the A^2/O - MBBR system (a: R=100%; b: R=200%; c: R=300%; d: R=400%; e, f: R=500%)

Fig.4 Nutrient variations in the typical anaerobic-anoxic/oxic batch tests on Day 40, Day 80, Day 125, Day 170, Day 215 (a - c: anaerobic stage; d - e: anoxic stage; f: oxic stage)

Fig.5 Microbial evolution of PAOs and GAOs (a - b, e - f, i - j: Total bacteria and targeting bacteria of PAO_{mix} on Day 40, Day 125, and Day 215, respectively; c - d, g - h, k - l: Total bacteria and targeting bacteria of GAO_{mix} on Day 40, Day 125, and Day 215, respectively; m: Distribution and comparison of PAOs and GAOs at different nitrate recycling ratios.) EUB_{mix} probe was shown in green while specific probe was in red.

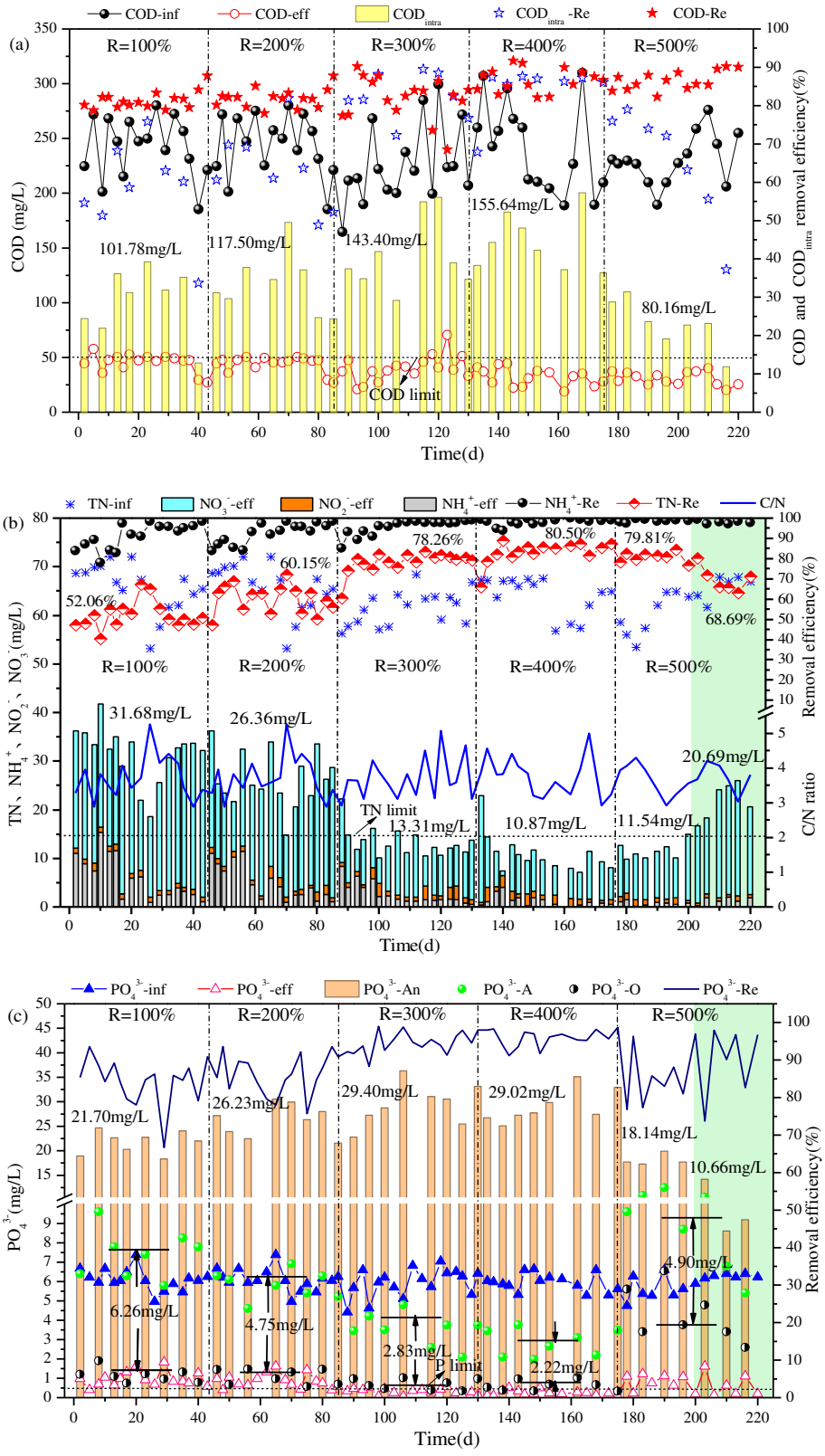

Fig.1 The overall removal performance in the A^2/O - MBBR system (a: COD; b: TN and NH_4^+; c: PO_4^{3-})

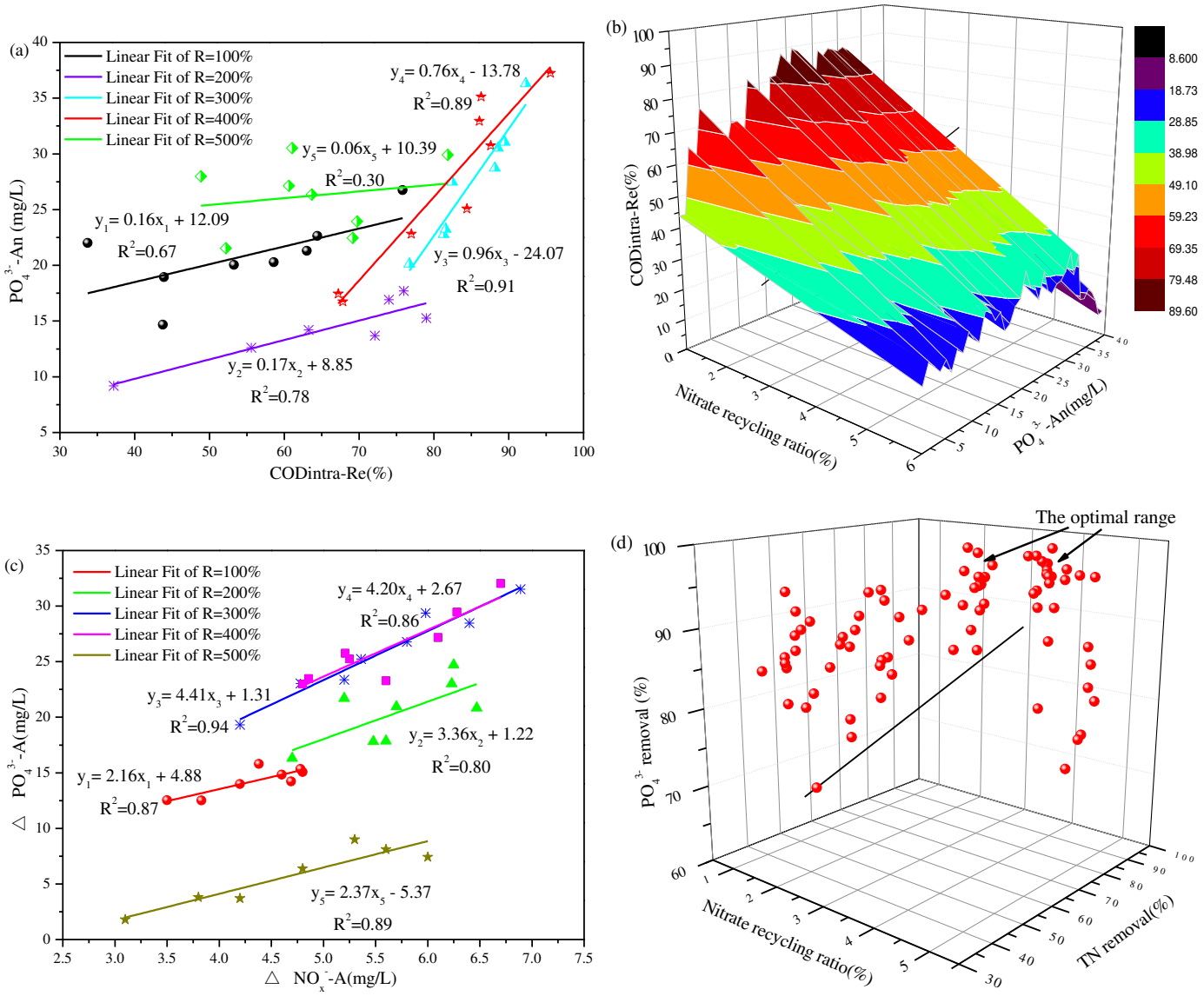

Fig.2 Correlation analysis of DPR characteristics (a, b: COD and PO_4^{3-}; c, d: TN and PO_4^{3-})

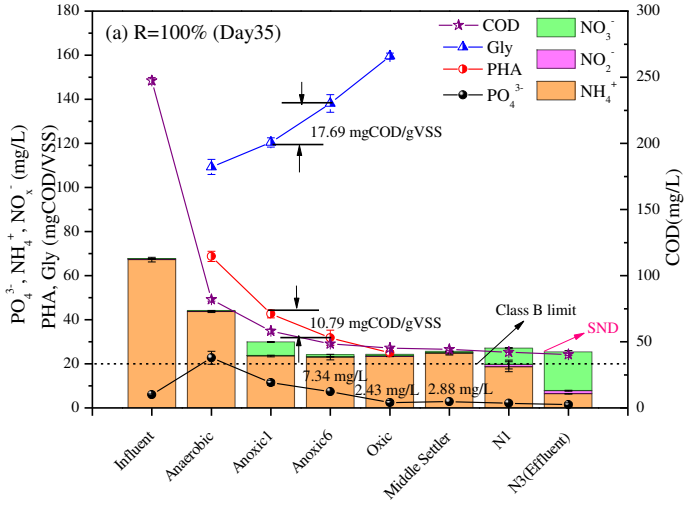
(a) R=100% (Day35)
COD
Gly
PHA
PO4 3-
NO3 -
NO2 -
NH4 +
17.69 mgCOD/gVSS
10.79 mgCOD/gVSS
Class B limit
SND
7.34 mg/L
2.43 mg/L
2.88 mg/L
PO4 3-, NH4 +, NOx - (mg/L)
PHA, Gly (mgCOD/VSS)
COD(mg/L)
Influent
Anaerobic
Anoxic1
Anoxic6
Oxic
Middle Settler
N1
N3(Effluent)

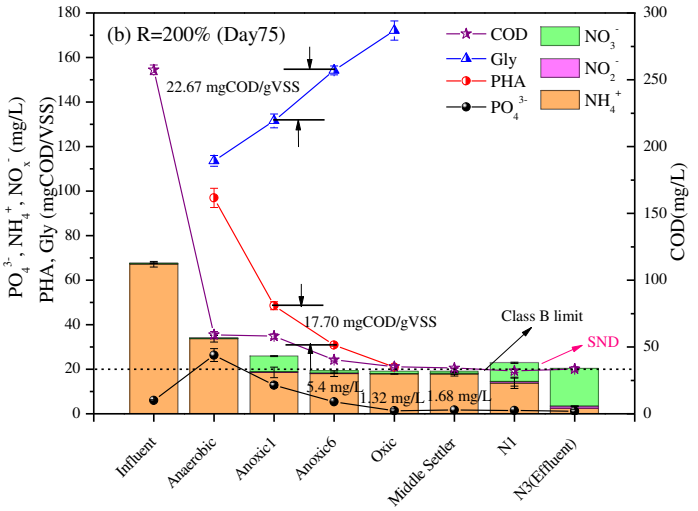
(b) R=200% (Day75)
COD
Gly
PHA
PO4 3-
NO3 -
NO2 -
NH4 +
22.67 mgCOD/gVSS
17.70 mgCOD/gVSS
Class B limit
SND
5.4 mg/L
1.32 mg/L
1.68 mg/L
PO4 3-, NH4 +, NOx - (mg/L)
PHA, Gly (mgCOD/VSS)
COD(mg/L)
Influent
Anaerobic
Anoxic1
Anoxic6
Oxic
Middle Settler
N1
N3(Effluent)

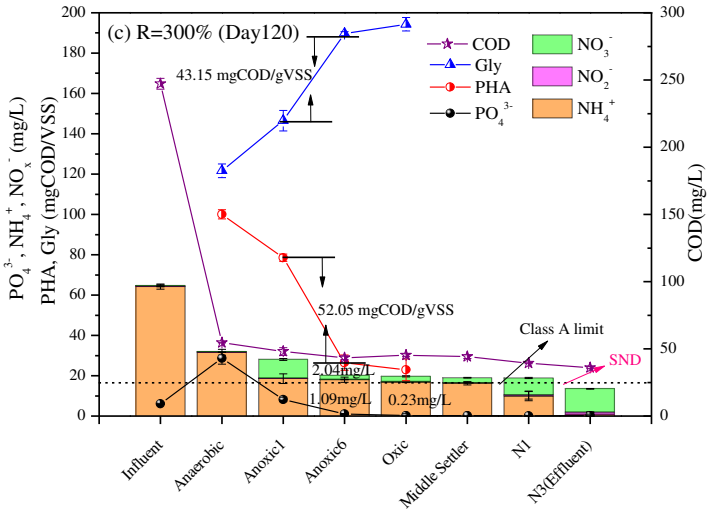
(c) R=300% (Day120)
COD
Gly
PHA
PO4 3-
NO3 -
NO2 -
NH4 +
43.15 mgCOD/gVSS
52.05 mgCOD/gVSS
Class A limit
SND
2.04mg/L
1.09mg/L
0.23mg/L
PO4 3-, NH4 +, NOx - (mg/L)
PHA, Gly (mgCOD/VSS)
COD(mg/L)
Influent
Anaerobic
Anoxic1
Anoxic6
Oxic
Middle Settler
N1
N3(Effluent)

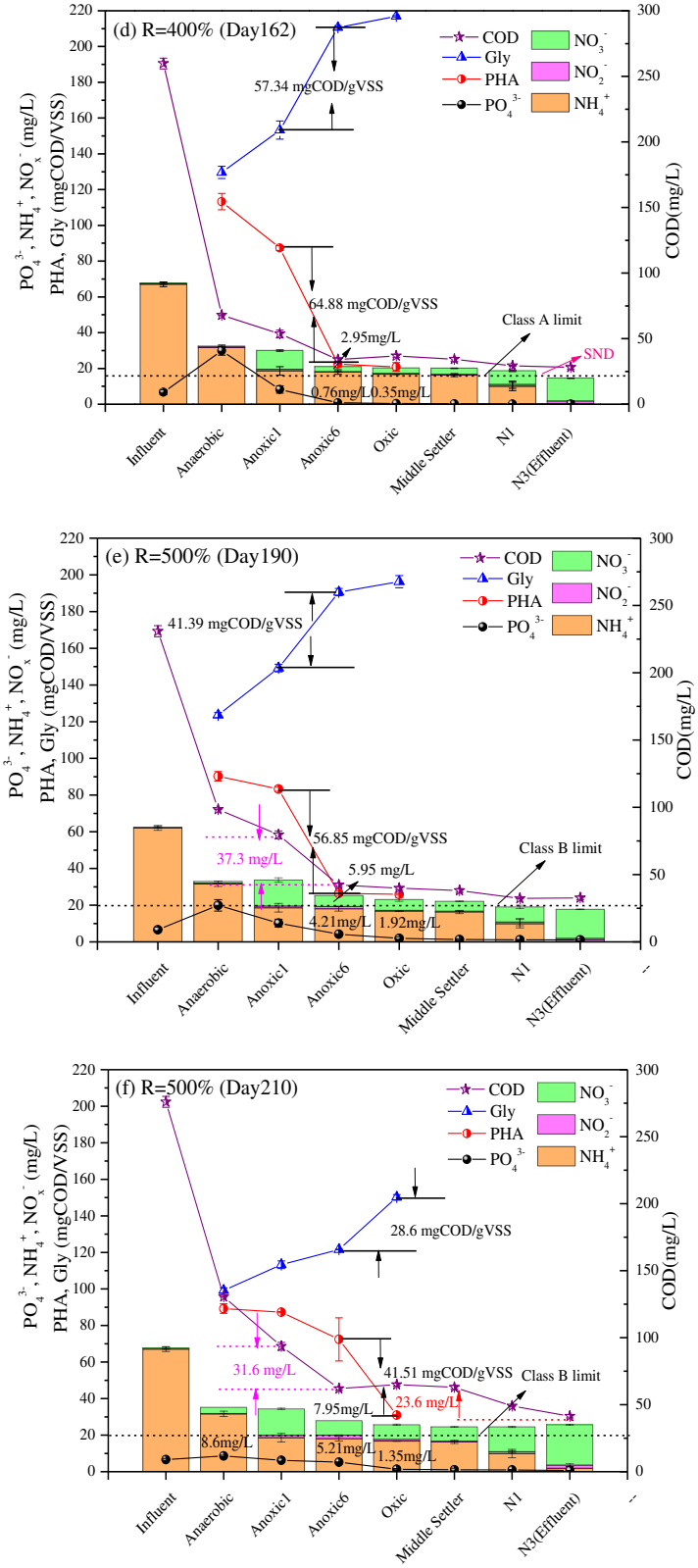

Fig.3 Nutrient variations along the reaction zones in the A^2/O - MBBR system (a: R=100%; b: R=200%; c: R=300%; d: R=400%; e, f: R=500%)

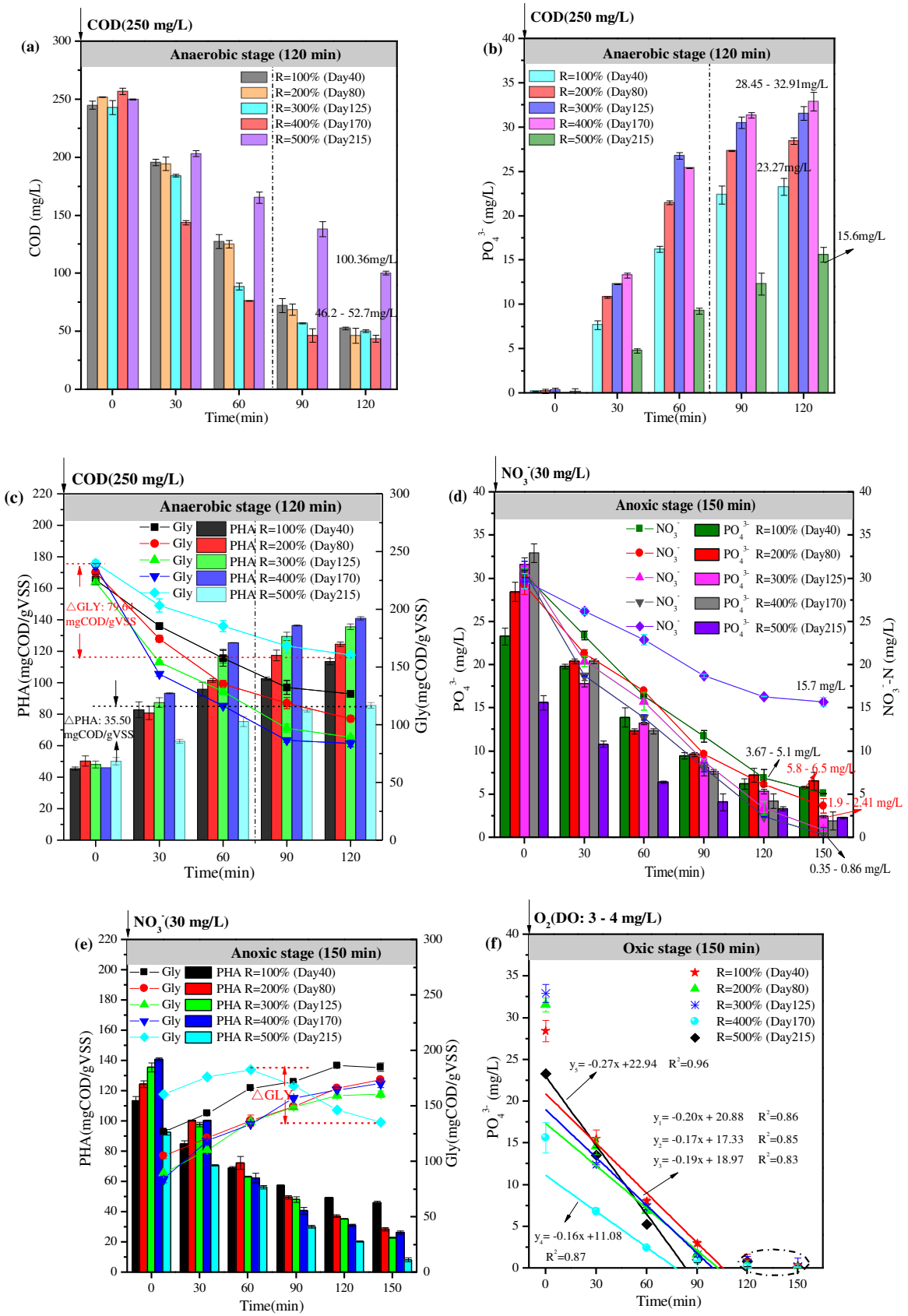

Fig.4 Nutrient variations in the typical anaerobic-anoxic/oxic batch tests on Day 40, Day 80, Day 125, Day 170, Day 215 (a - c: anaerobic stage; d - e: anoxic stage; f: oxic stage)

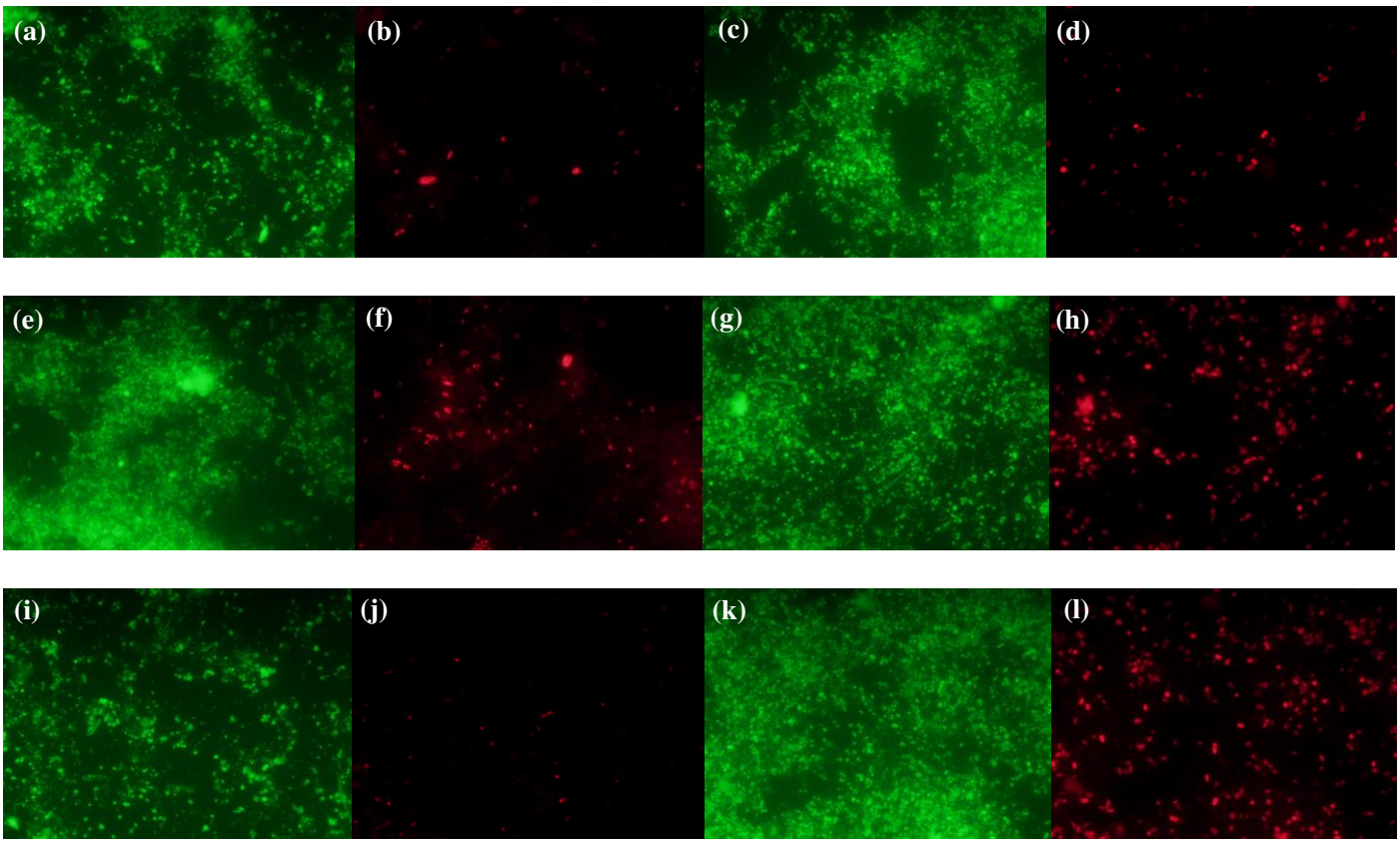

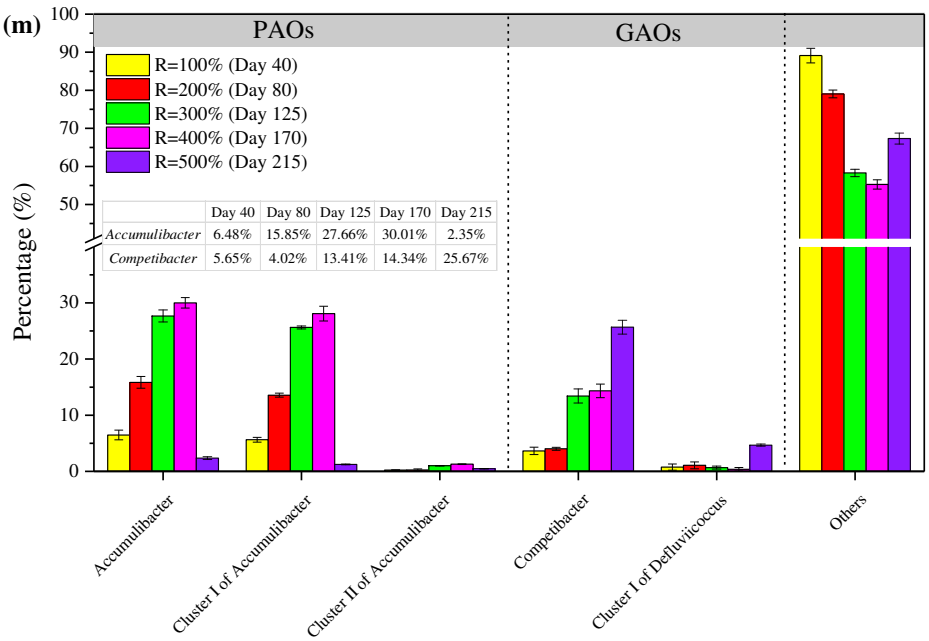

	Day 40	Day 80	Day 125	Day 170	Day 215
Accumulibacter	6.48%	15.85%	27.66%	30.01%	2.35%
Competibacter	5.65%	4.02%	13.41%	14.34%	25.67%

Fig.5 Microbial evolution of PAOs and GAOs (a - b, e - f, i - j: Total bacteria and targeting bacteria of PAO_{mix} on Day 40, Day 125, and Day 215, respectively; c - d, g - h, k - l: Total bacteria and targeting bacteria of GAO_{mix} on Day 40, Day 125, and Day 215, respectively; m: Distribution and comparison of PAOs and GAOs at different nitrate recycling ratios.) EUB_{mix} probe was shown in green while specific probe was in red.

Highlights:

1. PO_4^{3-}-An strongly depended on COD_{intra}-Re at R=300% (R^2=0.91) and R=400% (R^2=0.89).

2. Lower R inspired secondary P release, while higher R inhibited DPAOs activity.

3. R=300 - 400% allowed optimal PHA transformation, superior DPR and higher bioactivity.

4. Functional contribution of PAOs and GAOs was analyzed by stoichiometry methodology.

5. *Accumulibacter* (mainly Cluster I) outcompeted *Competibacter* with proper NO_3^- loading.

Graphical Abstract

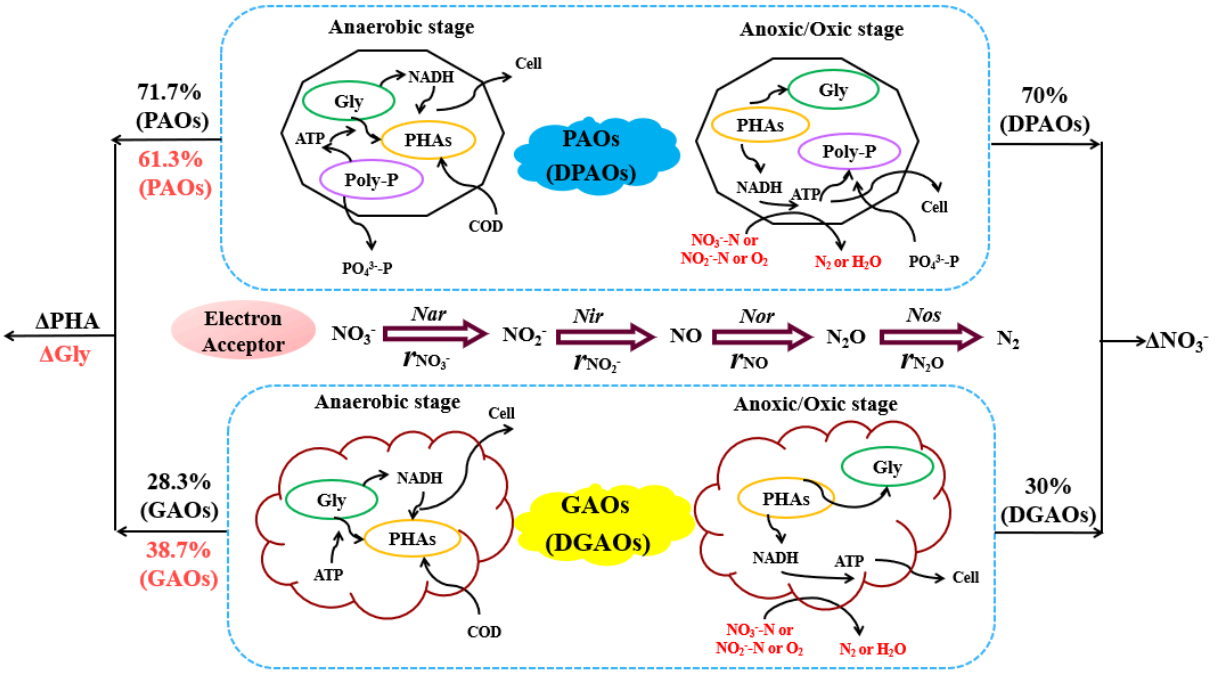

Supporting Information:

Roles of nitrate recycling ratio in the A^2/O - MBBR denitrifying phosphorus removal system for high-efficient wastewater treatment: performance comparison, nutrient mechanism and potential evaluation

Miao Zhang[a], Tianxin Song[a], Chenjie Zhu[a], Yajun Fan[b], Ana Soares[c], Xiaodan Gu[d], Jun Wu[a*]

[a] *College of Environmental Science and Engineering, Yangzhou University, Yangzhou 225127, PR China*

[b] *Yangzhou Polytechnic Institute, Yangzhou 225127, PR China*

[c] *Water Sciences Institute, Cranfield University, Cranfield, MK 43 0AL, UK*

[d] *School of Environmental Science and Engineering, Suzhou University of Science and Technology, Suzhou 215009, China*

*Corresponding author. Tel.: +86 15205278805. E-mail: j.wu@yzu.edu.cn (J. Wu)

Supporting information: 1 Figure and 1 Table.

Fig. S1 was used to point to Section 2.1.

Table S1 was used to point to Section 3.2.1.

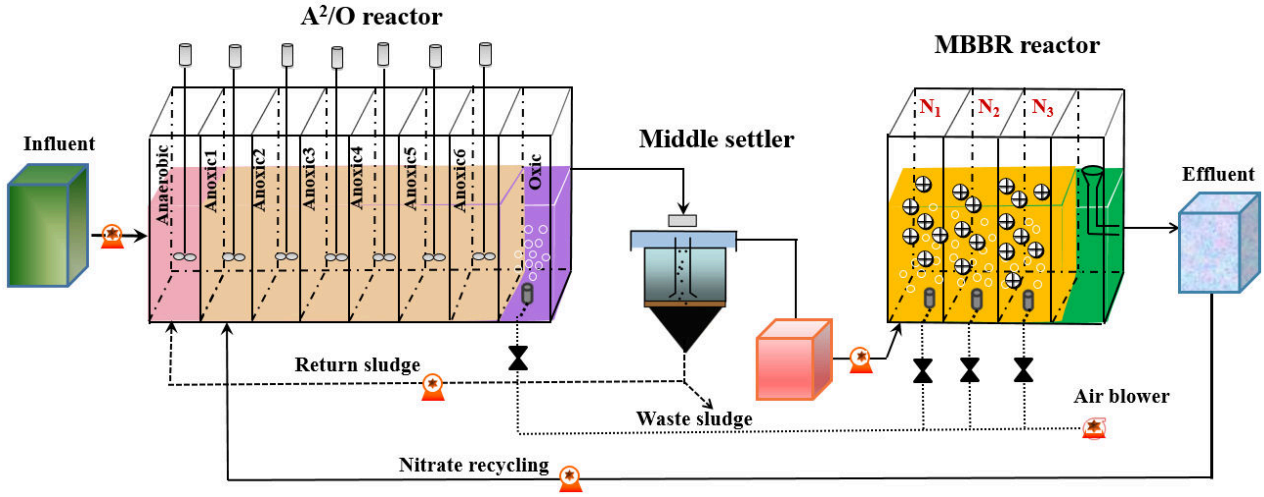

Fig. S1 Schematic diagram of the A^2/O - MBBR system

Table S1 Summary of DPR characteristics in the typical anaerobic-anoxic/oxic batch tests

Batch tests	Anaerobic stage (120 min)			Anoxic stage (150 min)			Oxic stage (150 min)		DPAOs /PAOs
	CUR mgCOD/(gVSS·h)	PRR mgP/(gVSS·h)	ΔPHA_{An}[c] (mgCOD/gVSS)	NDR mgN/(gVSS·h)	PUR_A mgP/(gVSS·h)	ΔPHA_A[c] (mgCOD/gVSS)	PUR_O mgP/(gVSS·h)	ΔPHA_O[c] (mgCOD/gVSS)	(%)
Phase1 (Day40)	37.87[a]/22.82[b]	5.18[a]/2.27[b]	50.50[a]/17.5[b]	3.28	2.25	67.60	4.80	73.05	46.9
Phase2 (Day80)	40.94/24.16	6.86/2.45	53.27/22.97	3.45	2.83	95.56	4.08	93.60	69.4
Phase3 (Day125)	49.78/13.71	8.18/1.54	68.85/15.53	3.91	3.76	112.75	4.56	120.35	82.5
Phase4 (Day170)	58.29/17.35	8.53/2.03	79.35/18.68	3.93	3.90	114.51	4.17	123.06	93.5
Phase5 (Day215)	27.26/21.01	2.95/2.05	25.20/10.30	1.81	1.72	84.34	4.93	92.30	34.9

a, b: the rates of the first and the last 60 min in the anaerobic stage;

c: PHA synthesis amount in the anaerobic stage, ΔPHA_{An}; PHA consumption amount in the anoxic stage, ΔPHA_A; PHA consumption amount in the oxic stage, ΔPHA_O.